Progress In Electromagnetics Research Letters, Vol. 49, 15–22, 2014

Two-dimensional Discretized Coherent Noise Jamming Method to Wideband LFM Radar

Shixian Gong[1, *], Xizhang Wei[1], Xiang Li[1], and Yongshun Ling[2]

Abstract—For coherent jammers to wideband linear frequency modulation (LFM) radar, the ratio between jamming energy and signal energy is always constant. To enhance the jamming to signal ratio (JSR), a two-dimensional (2D) discretized coherent noise jamming (2D-DCNJ) method is first proposed in this paper, where the covering area of the noise jamming results in 2D imaging is limited to a certain shape and further discretized to centralize the jamming energy. Moreover, the idea of weighting is applied to 2D-DCNJ to control the distribution of jamming energy, which can present some particular deceptive characteristics. The relationship between jamming results and modulated noise is analyzed, based on which the procedure of generating the jamming signal is detailed, and the JSR performance is compared with the previous ones. Finally, the validity of the proposed method is demonstrated via numerical simulation.

1. INTRODUCTION

Wideband linear frequency modulation (LFM) radar plays an important role in electronic reconnaissance, space surveillance and missile defense system for their capability of generating high-resolution one-dimensional (1D) or two-dimensional (2D) images of the targets [1, 2]. Therefore, the research of active jamming methods for countering wideband LFM radar is of great importance [3, 4], which can be mainly distributed into two classes: deception jamming and suppression jamming [5]. Because these techniques are always military secrets, there are actually few published materials. As an active suppression jamming method, traditional non-coherent noise jamming (non-CNJ) [6] cannot well counter to the wideband LFM radar for its poor relativity with the radar signal. By transmitting the product [7–9] or the convolution results [10, 11] of noise and radar signal, the coherence is improved, which can greatly enhance the output jamming to signal ratio (JSR). These methods are named as coherent noise jamming (CNJ) or smart noise jamming. However, only the 1D range coherence between the jamming signal and the radar signal is considered. In [12], a 2D coherent noise jamming method (2D-CNJ) to synthetic aperture radar (SAR) is presented to increase both the range and cross-range correlation between the jamming signal and the radar signal, which provides a new idea to improve the output JSR.

In this paper, a 2D discretized coherent noise jamming (2D-DCNJ) method to the wideband LFM radar is proposed, which can provide a great improvement on the output JSR of the 2D imaging results. By limiting and discretizing the covering area of the noise jamming results in 2D imaging, the jamming energy can be centralized. Moreover, by selecting a proper weighting function, the distribution of jamming energy can be further controlled to present some particular deceptive characteristics. The paper is organized as follows. Section II presents the principle of the 2D-DCNJ method, which illuminates the relationship between jamming results and modulated noise. Then the detailed procedure of the jamming

Received 3 July 2014, Accepted 10 August 2014, Scheduled 8 September 2014

* Corresponding author: Shixian Gong (gsx263642571@nudt.edu.cn).

[1] Research Institute of Space Electronics Information Technology, School of Electronic Science and Engineering, National University of Defense Technology, Changsha 410073, China. [2]Electronic Engineering Institute, Hefei 410073, China.

signal generation is presented in Section III, and the JSR performance of 2D-DCNJ is analyzed as well. In Section IV some numerical simulations are performed to prove the validity of the proposed method. Finally, we draw some conclusions in the last section.

2. PRINCIPLE OF 2D COHERENT NOISE JAMMING

LFM signal is commonly used in the wideband imaging radar systems. Traditionally, the stretch processing is applied to process extremely high bandwidth LFM waveforms [13, 14], which retains range resolution but restricts range coverage to a narrow window [15, 16].

2.1. Signal Processing Progress for Wideband LFM Radar

Assume that the transmitted signal is

$$s_{trans}(\hat{t}, t_m) = rect(\hat{t}) e^{j2\pi\left(f_c t + \frac{1}{2}\gamma \hat{t}^2\right)} \tag{1}$$

where $rect(\hat{t}) = 1$ for $|\hat{t}| \leq T_p/2$ and zero otherwise, $T_p/2$ is the pulse width, γ the chirp rate, f_c the radar carrier frequency, $\hat{t}$ the fast time, t_m the slow time, T the pulse repeat interval, m an integer, and $B = \gamma T_p$ the bandwidth of the signal. The reference signal is

$$s_{ref}(\hat{t}, t_m) = rect_{ref}(\hat{t}) e^{j2\pi\left[f_c\left(t - \frac{2R_{ref}}{c}\right) + \frac{1}{2}\gamma\left(\hat{t} - \frac{2R_{ref}}{c}\right)^2\right]} \tag{2}$$

where $rect_{ref}(\hat{t}) = 1$ for $|\hat{t}| \leq T_{ref}/2$ and zero otherwise, c is the velocity of light, and R_{ref} is the reference range.The impulse response of the low pass filtering (LPF) is supposed to be $h(\hat{t})$, and its spectrum is $H(f) = 1$ for $|f| \leq f_{stop}$ and zero otherwise, where f_{stop} is the cut-off frequency of the LPF.

Suppose that the translational motion is accurately compensated, and then the flow of wideband LFM radar signal processing can be illustrated as the block diagrams shown in Figure 1.

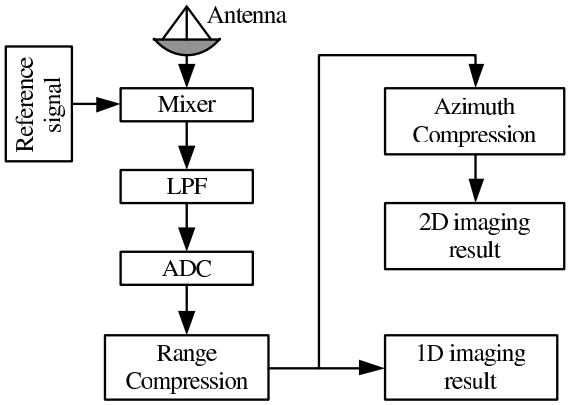

Figure 1. Signal processing block diagram of wideband LFM radar based on Stretch processing.

2.2. Signal Processing for the 2D-CNJ Method

The transmitted jamming signal of the 2D-CNJ method can be described as

$$\begin{aligned} J(\hat{t}, t_m) &= s_{trans}\left(\hat{t} - \frac{R_{jm}}{c}, t_m\right) \cdot n(\hat{t}, t_m) \\ &= rect\left(\hat{t} - \frac{R_{jm}}{c}\right) e^{j2\pi\left[f_c\left(t - \frac{R_{jm}}{c}\right) + \frac{1}{2}\gamma\left(\hat{t} - \frac{R_{jm}}{c}\right)^2\right]} \cdot n(\hat{t}, t_m) \end{aligned} \tag{3}$$

where R_{jm} is the distance between radar and jammer and $n(\hat{t}, t_m)$ the multiplied noise at the time t_m. According to the range compression method of the wideband LFM radar, we first achieve the product of the jamming signal and the conjugate reference signal as

$$\begin{aligned} J_{if}(\hat{t}, t_m) &= J\left(\hat{t} - \frac{R_{jm}}{c}, t_m\right) \cdot s_{ref}(\hat{t}, t_m)^* \\ &= rect\left(\hat{t} - \frac{2R_{jm}}{c}\right) \cdot n\left(\hat{t} - \frac{R_{jm}}{c}, t_m\right) \\ &\quad \cdot e^{-j\frac{4\pi}{c}\gamma\left(\hat{t} - \frac{2R_{ref}}{c}\right)R_{\Delta jm}} \cdot e^{-j\frac{4\pi}{c}f_c R_{\Delta jm} + j\frac{4\pi\gamma}{c^2}R_{\Delta jm}^2} \end{aligned} \tag{4}$$

where $R_{\triangle jm} = R_{jm} - R_{ref}$, and * denotes the complex conjugate. It can be seen that the bandwidth of $J_{if}(\hat{t}, t_m)$ is decided by that of $n(\hat{t}, t_m)$ and its position in the whole spectrum is determined by $f_j = -\frac{2\gamma R_{\triangle jm}}{c}$.

In 2D-CNJ methods, because the bandwidth of $n(\hat{t}, t_m)$ is limited, the frequencies of $J_{if}(\hat{t}, t_m)$ can be set smaller than f_{stop}, which guarantees that the jamming signal will not be filtered. After the Fast Fourier Transform (FFT), the 1D imaging result of jamming signal can be represented as

$$J_{1\mathrm{D}}(\hat{f}, t_m) = \left\{T_p sinc\left[T_p\left(\hat{f} - f_j\right)\right] \otimes N\left(\hat{f}, t_m\right)\right\} \cdot e^{-j\left(\frac{4\pi f_c}{c}R_{\Delta jm} + \frac{4\pi\gamma}{c^2}R_{\Delta jm}^2 + \frac{4\pi f_{rj}}{c}R_{\Delta jm}\right)} \tag{5}$$

where $N(\hat{f}, t_m)$ is the spectrum of $n(\hat{t}, t_m)$ along fast time and $\otimes$ represents the convolution operation.

For 2D imaging, $J_{1\mathrm{D}}(\hat{f}, t_m)$ is further multiplied with $e^{-j\pi\hat{f}^2/\gamma}$, and then the the 1D imaging result of jamming signal can be rewritten as [16]

$$J_{1\mathrm{D}}(\hat{f}, t_m) = \left\{T_p sinc\left[T_p(\hat{f} - f_j)\right] \otimes N(\hat{f}, t_m)\right\} \cdot e^{-j\frac{4\pi}{c}f_c R_{\triangle jm}} \tag{6}$$

By performing FFT of $J_{1\mathrm{D}}(\hat{f}, t_m)$ along slow time, the 2D imaging result of jamming signal can be obtained as

$$\begin{aligned} J_{2\mathrm{D}}(\hat{f}, f_m) &= \int_{-\infty}^{+\infty} rect(t_m) J_{1\mathrm{D}}(\hat{f}, t_m) e^{-j2\pi f_m t_m} dt_m \\ &= T_p \int_{-\infty}^{+\infty} sinc\left[T_p(\hat{f} - f'' - f_j)\right] \int_{-\infty}^{+\infty} rect(t_m) N(f'', t_m) \cdot e^{-j\frac{4\pi}{c}f_c R_{\Delta jm}} e^{-j2\pi f_m t_m} dt_m df'' \\ &= T_p T_m \left\{sinc\left[T_p(\hat{f} - f_j)\right] sinc\left[T_m(f_m - f_{jc})\right]\right\} \otimes_2 N(\hat{f}, f_m) \end{aligned} \tag{7}$$

where $\otimes_2$ represents the 2D convolution operation, f_{jc} the cross Doppler frequency of the jammer, and $N(\hat{f}, f_m)$ the 2D spectrum of $n(\hat{t}, t_m)$.

In order to express the relationship between the noise spectrum and the jamming results more clearly, the *sinc* function is approximated by the impulse function δ. Thus the 1D and 2D imaging results of the jamming can be respectively written as

$$\begin{cases} J_{1\mathrm{D}}(\hat{f}, t_m) = N(\hat{f} - f_j, t_m) \\ J_{2\mathrm{D}}(\hat{f}, f_m) = N(\hat{f} - f_j, f_m - f_{cj}) \end{cases} \tag{8}$$

As the jamming and signal have the same energy gain during the signal processing, the ratio of total jamming energy to signal energy is constant. So, if the covering area of jamming in images is reduced, the output JSR will be increased, which will be further explained in the next section. Equation (8) illustrates that the 1D and 2D jamming images depend on the corresponding spectrum of the multiplied noise. Therefore, by diminishing the frequencies component of the multiplied noise, the covering area can be reduced.

3. 2D DISCRETIZED COHERENT NOISE JAMMING METHOD

From Section 2 , it can be seen that a desired noise jamming result and an improvement of the JSR can be obtained by controlling the frequencies of the multiplied noise. Thus, we will propose a 2D-DCNJ method here.

3.1. 2D-DCNJ Method

As mentioned in the last section, the jamming results depend on the spectrum of the multiplied noise, so we can firstly generate the 2D random data, based on which the 2D spectrum of the multiplied noise can be generated by windowing, discretizing and weighting. Finally, by performing the 2D inverse Fast Fourier Transform (IFFT) to the spectrum, the multiplied noise used in 2D-DCNJ can be generated. The block diagram of 2D-DCNJ is shown in Figure 2 and its executing steps are given as follows.

Step 1: Generate the 2D random data $M(n,m)$, and set it as the 2D spectrum data.

Step 2: Create a 2D window function $w(n,m)$, which can both limit the area and control the energy distribution. Multiply $M(n,m)$ by $w(n,m)$

$$R(n,m) = M(n,m) \cdot w(n,m) \tag{9}$$

Step 3: Set a 2D random coordinate subset Q of the data plane, and the 2D discretizing function can be given by

$$H\left(n,m\right) = \begin{cases} 1 & (n,m) \in Q \\ 0 & (n,m) \notin Q \end{cases} \tag{10}$$

Then, the 2D spectrum of the multiplied noise is the product of $R(n,m)$ and $H(n,m)$, which can be described as

$$N_f(n,m) = R(n,m) \cdot H(n,m) \tag{11}$$

Step 4: By performing the 2D IFFT of $N_f(n,m)$, the multiplied noise of the 2D-DCNJ method can be generated.

Step 5: Finally, after the up conversion, the transmitting jamming signal of the 2D-DCNJ method can be finally generated.

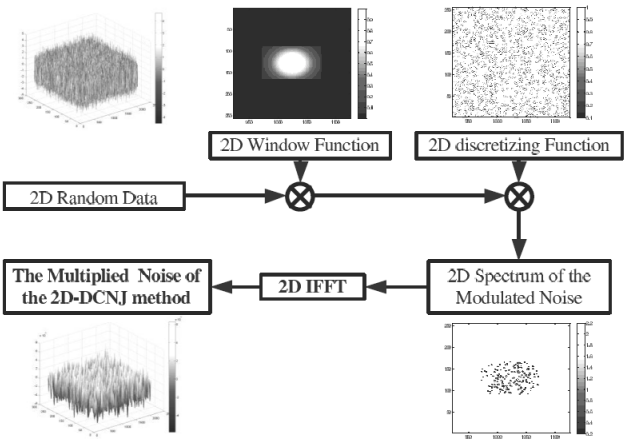

Figure 2. The generation of multiplied noise for the 2D-DCNJ method.

3.2. JSR Performance of 2D-DCNJ Method

For traditional non-CNJ methods, the bandwidth of $J_{if}(\hat{t}, t_m)$ is always larger than f_{stop}. Then, after LPF, the energy ratio between jamming and signal is

$$E\_JSR_1 = \frac{2f_{stop}}{B_{Non}} E\_JSR_0 \tag{12}$$

where B_{Non} is the bandwidth of $J_{if}(\hat{t}, t_m)$ and E_JSR_0 the input energy ratio of jamming to signal. The input JSR can be represented as

$$JSR_0 = E\_JSR_0 \frac{T_s}{B_{T_J}} \tag{13}$$

where T_s is the time width of signal and T_J the time width of jamming signal which is usually the same as T_s . The covering area of the non-CNJ method is the whole imaging area A_{all}. Then the relationship between the input and output JSR can be expressed as

$$NCNJ\_JSR_{output} = E\_JSR_1 \frac{A_s}{B_{A_{all}}} = JSR_0 \frac{A_s}{B_{A_{all}}} \cdot \frac{2f_{stop}}{B_{Non}} \tag{14}$$

where A_s is the covering area of target signal.

For the coherent jamming methods, such as CNJ method and false target jamming method, the bandwidth of $J_{if}(\hat{t}, t_m)$ is smaller than f_{stop}. Then, the energy ratio between jamming and signal is constant. The relationship between the input and output JSR can be described as

$$CNJ\_JSR_{output} = E\_JSR_0 \frac{A_s}{B_{A_J}} = JSR_0 \frac{A_s}{B_{A_J}} \tag{15}$$

where A_J is the covering area of jamming signal.

It can be seen from (14) and (15) that the JSR performance is mainly determined by the covering area of jamming signal. The trend of JSR performance for different active jamming methods such as commonly CNJ method, 2D-CNJ method, 2D-DCNJ method and false target jamming method is presented in Figure 3.

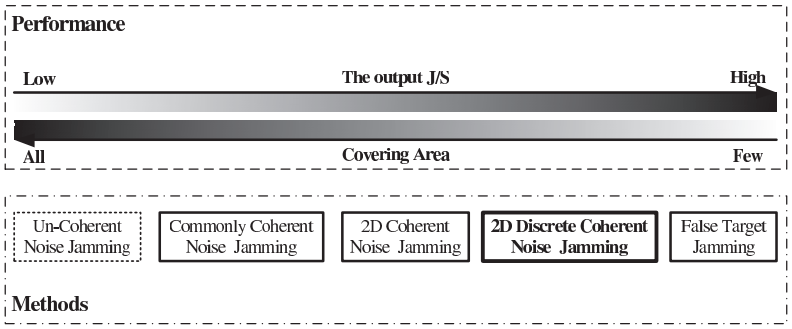

Figure 3. Comparison of the active jamming methods.

Because the spectrum of the multiplied noise is highly centralized, the proposed 2D-DCNJ method can greatly improve the JSR performance. Firstly, by windowing, the jamming area is limited and the energy distribution is controlled. Secondly, with the 2D discretizing function, the jamming area is further reduced to give a great increase to the output JSR. Therefore, the proposed 2D-DCNJ can provide the best JSR performance among the noise jamming methods. It should be stated that as the shape and the energy distribution of the window function can be designed similar to a target, the 2D-DCNJ method has the potential of deception jamming, and it will become false target jamming method if the 2D discretizing function is set to be several given points.

4. SIMULATION

In this section, some simulations are performed with a wideband LFM ISAR system, and the target used is an ideal point scattering, which can provide the highest output power. The parameters are illustrated in Table 1.

Table 1. Simulation parameters.

Parameter	Value	Parameter	Value
Sampling frequency	20 MHz	B	1 GHz
The location of Radar	(0 m, 0 m)	T	1 ms
The location of Jammer	(0 m, 10000 m)	T_p	10 μs
The location of Target	(10 m, 10002 m)	f_c	10 GHz
Angular velocity	$\pi/20$ rad/s	f_{stop}	10 MHz

4.1. Simulation of Different Noise Jamming Methods

By setting the input JSR as 20 dB, the 2D imaging results of the non-CNJ method, commonly CNJ method, 2D-CNJ method and the proposed 2D-DCNJ method are respectively shown in Figure 4.

From Figure 4(a), we can see that the non-CNJ method performs poorly when countering to the wideband LFM radar, although the bandwidth of jamming signal is the same as the radar signal which can bring a best jamming performance according to the theory of traditional noise jamming. Figure 4(b) and Figure 4(c) demonstrate that the output JSR of CNJ methods can be improved by reducing the covering area. However, the target can still be found. It can be seen from Figure 4(d) that with the proposed 2D-DCNJ method the target is masked by the jamming signals, which proves that the JSR can be greatly improved by limiting and discretizing of the covering area. Besides, the suppression jamming area of the 2D-DCNJ method is almost the same as that of 2D CNJ method. Therefore, we can conclude that the 2D-DCNJ method performs much better than the other ones.

In order to compare the performance of the methods more quantitatively, the output JSR of simulation result as well as the calculated results in theory for each jamming method is presented in Table 2 , from which we can also see that the output JSR can be improved by reducing the covering area and the 2D-DCNJ method performs the best.

Table 2. The JSR Performance of different methods.

	Non-CNJ	Commonly CNJ	2D-CNJ	2D-DCNJ
Output JSR of Simulation (dB)	−40.9210	−20.9818	−15.8936	−10.0248
Output JSR in theory (dB)	−41.0721	−21.0721	−15.8433	−9.9087

4.2. Further Analysis of the 2D-DCNJ Method

By 2D-CNJ and 2D-DCNJ methods, the 2D imaging results of jamming are obtained with cone-shaped jamming area (as shown in Figure 5) when the input JSR is 20 dB. For the energy distribution of the jamming results is non-uniform, this paper just gives the output peak power ratios between jamming and signal, which are 6.7111 dB in Figure 5(a) and 9.3264 dB in Figure 5(b). From the output peak power ratios, we can see that a greater JSR improvement of the 2D-DCNJ method can be achieved when compared with the 2D-CNJ method.

The non-uniform energy distribution characteristics of the results in Figure 5 show that the 2D-DCNJ method has the characteristic of deception jamming for it can simulate the reflection coefficient characteristic of target. Moreover, it can be seen from Figure 5 that whit certain shaped jamming area 2D-DCNJ method has the shape characteristic of deception jamming.

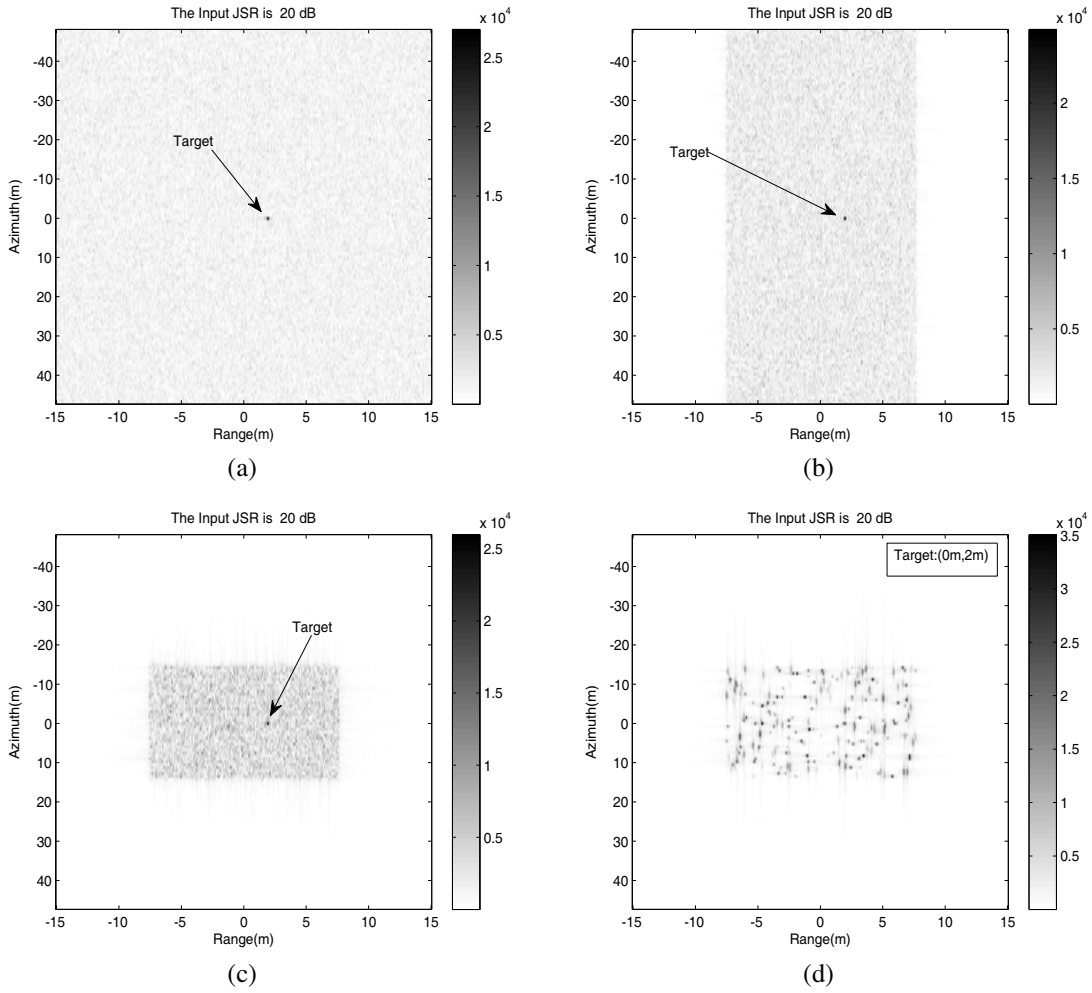

Figure 4. 2D imaging results with jamming. (a) non-CNJ method; (b) Commonly CNJ method; (c) 2D-CNJ method; (d)The 2D-DCNJ method.

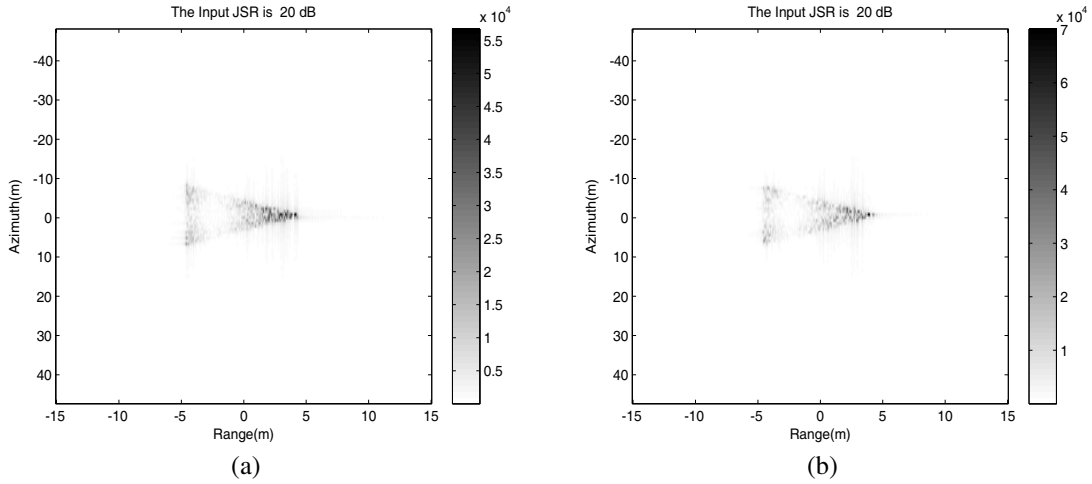

Figure 5. The 2D imaging results with jamming cone-shaped area. (a) 2D-CNJ method. (b) The 2D-DCNJ method.

5. CONCLUSIONS

In this paper, a 2D-DCNJ method to the wideband LFM radar is proposed. The principle and procedure of generating the jamming signal are presented as well as the JSR performance comparison. Simulation results demonstrate that the 2D-DCNJ method can achieve much higher JSR due to the deduction of covering area in 2D imaging and present some deceptive characteristics by applying particular 2D window functions.

REFERENCES

1. Chen, V. C. and H. Ling, *Time-Frequency Transforms for Radar Imaging and Signal Analysis*, Artech House, Norwood, MA, 2002.
2. Park, J. I. and K. T. Kim, "A comparative study on ISAR imaging algorithms for radar target identification," *Progress In Electromagnetics Research*, Vol. 108, 155–175, 2010.
3. Liu, Q., S. Xing, X. Wang, J. Dong, D. Dai, and Y. Li, "The interferometry phase of InSAR coherent jamming with arbitrary waveform modulation," *Progress In Electromagnetics Research*, Vol. 124, 101–118, 2012.
4. Liu, Q., J. Dong, X. Wang, S. Xing, and B. Pang, "An efficient SAR jammer with direct radio frequency processing (DRFP)," *Progress In Electromagnetics Research*, Vol. 137, 293–309, 2013.
5. Li, N. J. and Y. T. Zhang, "A survey of radar ECM and ECCM," *IEEE Trans. AES*, Vol. 31, No. 3, 1110–1120, 1995.
6. Dumper, K., P. S Cooper, A. F Wonsl, et al., "Spaceborne synthetic aperture radar and noise jamming," *Proceedings of the 1997 Radar Edinburgh International Conf.*, 411–414, Edinburgh, UK, 1997.
7. Dong, C. X., S. Q. Yang, G. Q. Zhao, et al., "Effect of noise FM jamming against ISAR imaging," *CIE Int. Conf. Radar*, 1016–1018, Shanghai, China, 2006.
8. Wang, W. Q. and J. Y. Cai, "A technique for jamming bi- and multistatic SAR systems," *IEEE GRSL*, Vol. 4, No. 1, 80–82, 2007.
9. Lee, Y. J., J. R. Park, W. H. Shin, et al., "A study on jamming performance evaluation of noise and deception jammer against SAR satellite," *Proc. 2011 Int. APSAR Conf.*, 1–3, 2011.
10. Wei, Y., R. Hang, S. X. Zhang, et al., "Study of noise jamming based on convolution modulation to SAR," *Int. Conf. CMCE*, 169–172, Changchun, China, 2010.
11. Lv, B., "Simulation study of noise convolution jamming countering to SAR," *ICCDA*, V4130–V4133, Qinhuangdao, Hebei, China, 2010.
12. Feng, X. Z. and X. J. Xu, "A 2-D correlated noise depressive jamming technique to synthetic aperture radar," *IET Int. Radar Conf.*, 1–4, Guilin, China, 2009.
13. Bassem, R. M. and Z. E. Atef, *Matlab Simulations for Radar Systems Design*, Chapman Hall/CRC CRC Press LLC, 2004.
14. Ozdemir, C., *Inverse Synthetic Aperture Radar Imaging With MATLAB Algorithms*, John Wiley, Hoboken, New Jersey, 2012.
15. Camp, W. W., J. T. Mayhan, and R. M. O Donnell, "Wideband radar for ballistic missile defense and range-doppler imaging of satellites," *Lincoln laboratory Journal*, Vol. 12, No. 2, 267–280, 2000.
16. Bao, Z., M. D. Xing, and T. Wang, *Radar Imaging Technology*, Publishing House of Electronics Industry, Beijing, China, 2004.